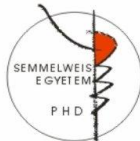


**The clinical value of CT angiography and brain MRI following
transcatheter aortic valve implantation
Ph.D. thesis**

Ferenc Imre Suhai MD

Doctoral School of Theoretical and Translational Medicine



Supervisor: Dr. Szilveszter Bálint

Official reviewers: Dr. Végh Eszter Mária, Ph.D
Dr. Nardai Sándor, Ph.D

Head of the Complex Examination Committee:

Members of the Complex Examination Committee:

Budapest
2023

1 INTRODUCTION

Aortic stenosis (AS) is the most common valvular disease in developed countries. Its prevalence significantly rises with increasing age and AS has a significant impact on both morbidity and mortality. Currently, the standard treatment for patients with severe AS is surgical aortic valve replacement (SAVR). However, transcatheter aortic valve implantation (TAVI) has emerged as a safe and effective alternative to SAVR in symptomatic patients with high or prohibitive risk and as a valid alternative to SAVR in patients with intermediate risk. TAVI has been recently expanded to lower risk patient population. As the indication for TAVI expands to lower-risk populations, it becomes increasingly important to consider the prognostic role of left ventricular remodelling and cerebrovascular events (CVE) in patients undergoing this procedure. With the potential for more patients to undergo TAVI, it is crucial to carefully evaluate the impact of the procedure on left ventricular reverse remodelling and the incidence of cerebrovascular events and effect on long term cognitive function which could have a significant impact on short and long-term morbidity and mortality. Therefore, understanding the prognostic significance of these factors will be essential in ensuring the continued success and safety of TAVI in lower-risk patient populations.

1.1 Left ventricular remodelling

AS leads to adaptational adverse cardiac remodelling due to chronic pressure overload of the LV (3). Left ventricular hypertrophy (LVH) is strongly associated with significant risk of cardiovascular mortality and morbidity regardless of its etiology (4, 5). Moreover, chronic pressure overload and subsequent remodelling are accompanied by diastolic and/or systolic LV dysfunction (6-9). LV reverse remodelling will occur immediately after the elimination of afterload (after surgical or transcatheter valve replacement), which means immediate improvement of cardiac function occurs, followed by beneficial reverse remodelling (LV mass regression) at medium- and long-term. According to the literature, the regression of LV mass (LVM) is a protective factor (15) and is associated with reduced hospitalization rate (16, 17).

1.2 Hypo-attenuated leaflet thickening

Hypo-attenuated leaflet thickening (HALT) of transcatheter aortic valve leaflets has been described on cardiac computed tomography angiography (CTA) datasets in patients after TAVI. HALT is considered an early imaging feature of subclinical leaflet thrombosis (SLT), which is a common finding after TAVI, the reported frequencies varying from 0.6% to 40%. HALT can develop despite established post-procedural antiplatelet regimens and, in many cases, may resolve completely

after the initiation of anticoagulation therapy. A previous study suggested that valve thickening or thrombosis is considered to have a significant impact on hemodynamic prosthetic valve deterioration, which has been linked with less LV reverse remodelling after aortic valve replacement. However, whether HALT affects LV reverse remodelling after TAVI and the clinical relevance of SLT is still under debate, some studies find increased risk for stroke or transient ischemic attack (TIA), whereas others did not find any associations between SLT and CVE.

1.3. Cerebral embolization and cerebrovascular events

Cerebrovascular events (CVE) following Transcatheter Aortic Valve Implantation (TAVI) are serious complications associated with significant short-term and long-term risks of morbidity and mortality. The incidence of CVE after TAVI varies widely in different studies, ranging from 1% to 11% according to the definitions. The Partner 3 trial, which examined TAVI as an alternative to surgical aortic valve replacement (SAVR) in low-risk patients with severe symptomatic aortic stenosis (AS), demonstrated that TAVI was superior to SAVR in reducing the composite endpoint of death from any cause or disabling stroke. Silent cerebral ischemic lesions (SCILs) are often found (58-91%) in cerebral magnetic resonance imaging (MRI) studies after TAVI, even though they may not manifest as overt strokes. These SCILs have been associated with potential cognitive impairment, dementia, cognitive decline, and depression. However, recent research has shown mixed results, with some subjects experiencing cognitive improvement despite the presence of new cerebral lesions. TAVI can influence cognitive function both positively and negatively.

Therefore, state-of-the-art cardiovascular imaging aims to provide accurate assessment HALT and reverse remodelling processes and to investigate cerebral lesion, cerebrovascular events and neurological consequences after TAVI.

2 OBJECTIVES

2.1 LV reverse remodelling

- To investigate independent predictors of reverse remodelling after TAVI and to assess the prognostic value of LV reverse remodelling on mortality and hospitalisation for heart failure.

2.2 Cerebral embolization and CVE after TAVI

- To define independent predictors of patient and procedural related predictors of ischemic lesion volume and stroke
- To evaluate the occurrence and distribution of ischemic brain lesions using diffusion MRI
- To assess the effect of SCILs on the patient's neurocognitive function

2.3 White matter microstructural changes between the discharge and 6 months brain MRI following TAVI

- To assess DTI metric changes in the corpus callosum and cingulum
- To correlate DTI metrics with postprocedural ischemic lesion volume (ILV) and evaluate the cognitive trajectory of subjects undergoing TAVI.

3 METHODS

3.1 Study population and design

3.1.1 Study population and design for the evaluation of reverse remodelling after TAVI

In a single center, prospective cohort study we analysed 117 consecutive patients who underwent CT angiography for pre-TAVI planning and were assessed following TAVI to determine the presence or absence of SLT as part of the RETORIC study (Rule out Transcatheter Aortic Valve Thrombosis with Post Implantation Computed Tomography trial, NCT02826200). As part of the standard clinical evaluation, pre-TAVI imaging was conducted to assess the aortic root anatomy and determine the appropriate access routes (iliofemoral and supraaortic arteries) for transcatheter heart valve sizing and TAVI eligibility. CTA imaging was also utilized to evaluate bioprosthetic valve function and LV morphology after TAVI. Follow-up echocardiography was performed on the same day to assess LV morphology at various time points following TAVI (average of 1.7 years)

3.1.2 Study population and design for the evaluation of procedural predictors of CVE and neurological consequences following TAVI

In a single-center, prospective cohort study, from 153 patients we analyzed 113 consecutive patients after exclusion who underwent CT angiography for pre-TAVI planning and brain MRI following TAVI and at six-month (6M) as part of the RETORIC study. The patients were followed up until 1 year.

3.1.3 Coronary Study population and design for DTI metric and microstructural WM changes

As a part of the previous study, we included subjects into the DTI substudy with complete and adequate discharge TAVI and 6M follow-up MRI datasets. The final DTI study cohort consisted of 78 participants. Inclusion criterion of the cognitive study was the accomplishment of the pre-TAVI baseline and at least one of the three

further neurocognitive tests (divided into “DTI cognitive” and “non-DTI cognitive” cohorts).

3.2 Left Image acquisition for TAVI planning and follow-up

We used the following CTA protocol for every pre-TAVI planning CT: first, we acquired a prospectively ECG triggered non-contrast scan from the entire heart (120 kV, slice thickness of 3 mm, increment 1.5 mm). This was followed by a retrospectively ECG-gated CTA of the aorta (from the level of thoracic inlet to the level of the femoral head), and the heart, during a single breath-hold, using a 256-slice CT scanner (Philips Healthcare, 270 msec rotation time, tube voltage of 100-120 kV based on body mass index) for TAVI planning. We administered 75 ml contrast agent with 4.5 ml/s flow, and images were acquired with 1 mm slice thickness, and 1 mm increment using iterative reconstruction (iDose4 and IMR, Philips Healthcare). Follow-up CT examinations were performed using retrospective gating with similar scan protocol, with shorter scan length covering.

3.3 Cardiac CTA image analysis

Two radiologists evaluated calcification in various parts of the aorta, including the aortic valve, annulus, left ventricular outflow tract, ascending aorta, and aortic arch, using qualitative grading (mild, moderate, severe) based on planning CTA images. Aortic valve calcium score (AVCS) was measured with the Agatston method on non-contrast cardiac CT scans, excluding extravalvular calcium. Left ventricular mass (LVM) was evaluated pre- and post-TAVI using semi-automated software (Heartbeat-CS, Philips Intellispace v6.0.4). LV reverse remodeling was defined as >20% reduction in LVM on post-TAVI CT scans.

Subclinical leaflet thrombosis (SLT) was assessed by three experienced radiologists on follow-up CT scans (average 1.7 years post-TAVI). Leaflets were examined individually, and leaflet thickness >3 mm indicated SLT.

3.4 Echocardiography Assessment Prior to the TAVI procedure and During Follow-up

We performed TTE for all 117 patients using an EPIQ 7C system (Philips Medical System, Andover, MA, USA), equipped with X5-1 matrix transducer. The 2D grey-scale images were recorded over three heart cycles and analysed using QLab software (version 10.0 Philips Medical System, Andover, MA, USA) by one of four experienced echocardiographers, blinded to the CT data. Transaortic peak and mean pressure gradients were calculated using the simplified Bernoulli equation. The change in mean pressure gradient was determined by calculating the difference between the pre-procedural pressure gradient values and those obtained during the follow-up period. Laboratory, imaging, and clinical data were evaluated at follow-up study visits by a cardiologist at the same day of CT and echocardiographic imaging.

3.5 Endpoint definition for adverse events in patients evaluated for LV reverse remodelling

We defined hospitalization for heart failure as any hospitalization event that lasted for >24 h during the follow-up period, at which patient demonstrated at least two heart failure-related symptoms (i.e. oedema and dyspnoea) and required intravenous diuretic therapy. To ensure the accuracy and integrity of mortality data, official death records from the National Health Insurance Fund were collected and carefully verified. This meticulous process aimed to prevent any loss of patient information during the follow-up period. Mean follow-up time was 2.6 years for this patient cohort. Composite endpoint was defined as heart failure hospitalization or all-cause mortality during follow-up. Survival time was calculated from the date of TAVI to the date of confirmed death, hospitalization or last contact with the patient. We compared clinical outcomes in patients with more and less than 20% reduction in LV mass (the definition of reverse remodelling).

3.6 TAVI procedure and periprocedural complications

In our study assessing the periprocedural risk factors and complications in 113 patients prosthetic valves were implanted with the standard technique, using local anesthesia with conscious sedation during the procedure. Transfemoral route was the preferred access, transsubclavian or transcarotid routes were considered as an alternative route. Embolic protection devices were not used in this cohort. Adverse events were defined according to the Valve Academic Research Consortium-3 definitions (VARC-3). Procedural factors such as balloon pre- and postdilations, the number of attempts to position and events of valve dislocation were evaluated and collected in a dedicated database.

3.7 Discharge- and follow-up MRI

We evaluated the periprocedural complications in 113 patients, we performed discharge brain MRI in the first week (4 days after TAVI on average) to detect cerebral ischemic lesions. The MRI examinations were performed on a 1.5T MR scanner (Achieva, Philips Medical Systems) using an 8-channel head coil after TAVI (referred to as discharge MRI). Fluid-Attenuated Inversion Recovery (FLAIR), T2-weighted, T2*-gradient echo, high resolution 3D T1-weighted gradient echo sequences were obtained with diffusion MRI. MRI was repeated at 6 months (6M) in order to assess the gliotic transformation of procedural ischemic lesions. Follow-up MRI examination was performed with the same protocol. Diffusion MRI acquisitions were performed using a single shot spin echo, echo-planar imaging sequence in 32 diffusion encoding directions with $b=800$ s/mm² and one $b=0$ measurement. Whole brain coverage was obtained with 2 mm-thick contiguous axial slices. From the diffusion MRI dataset averaged diffusion-weighted images commonly referred to as 'trace' and mean diffusivity and ADC maps were automatically derived and used to calculate the ischemic lesion volume (ILV).

3.8 Assessment of DTI metrics and white matter region of interests

Diffusion MRI data was processed using the ExploreDTI toolbox in Matlab. To correct distortions from patient motion and other factors, registration was performed by aligning diffusion-weighted images ($b = 800$) with the first $b = 0$ volume. This correction addressed motion artifacts and magnetic susceptibility-related distortions in a single step, with each subject's 3D T1-weighted images used for registration. Robust tensor fitting with outlier rejection was done, and average MD, AD, RD, and FA values were computed in regions of interest (ROIs) covering major white matter tracts on the corrected diffusion MRI data (Figure 1). The study included 78 subjects with complete and adequate discharge and 6-month follow-up MRI data. For white matter segmentation, the Johns Hopkins University WM tractography atlas was applied, and the atlas labels were transformed to individual image spaces using the Elastix software within ExploreDTI. Seven white matter ROIs were analyzed, and these were manually adjusted by an experienced neuroradiologist to exclude gray matter or cerebrospinal fluid contamination.

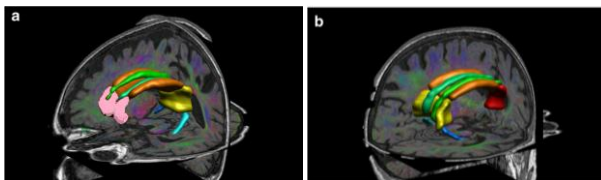


Figure 1. A 3D MR images of a subject's regions of interest projected over the fused colour coded fractional anisotropy and T1 weighted images.

3.9 Ischemic lesion volume measurement

The localisation, number and size in three perpendicular diameters of all lesions with restricted diffusion were recorded using a PACS workstation (Impax 6.5.2.657, Agfa HealthCare). ILV was calculated as the sum of lesion volumes using the formula of $a \times b \times c \times 0.52$ (a, b and c are the three lesion diameters) (83). The ILV measurements were performed in a random order and the investigator was blinded to the scan date and patient data.

In the DTI substudy based on ILV three groups were created as follows:

- Group I: patients with $ILV < 100 \text{ mm}^3$ (31 subjects).
- Group II: $100 \text{ mm}^3 < ILV < 300 \text{ mm}^3$ (25 subjects).
- Group III: $300 \text{ mm}^3 < ILV$ (22 subjects)

3.10 Neurocognitive assessment

Patients underwent a serial evaluation of the cognitive status pre-TAVI, post-TAVI before hospital discharge, 6M, and 1Y following TAVI. We used the Hungarian version of the Addenbrooke's Cognitive Assessment (ACE) test (84), which

incorporated the Mini Mental State Examination (MMSE), and the evaluation was performed by one of two trained investigators blinded to CTA and MRI data. Among all enrolled patients 113 participants completed the pre-TAVI, 83 subjects the post-TAVI, 93 subjects the 6M, finally 79 patients the 1Y cognitive tests. Patients with periprocedural stroke (6/113, 5.3%) were excluded from the further neurocognitive assessment. Inclusion criterion of the cognitive study was the accomplishment of the pre-TAVI baseline and at least one of the three further neurocognitive tests (divided into “DTI cognitive” and “non-DTI cognitive” cohorts).

3.11 Statistical analysis

Continuous variables are expressed as mean \pm standard deviation, while categorical variables are presented as frequency and percentages. Chi-squared tests were used for comparing categorical variables, and Wilcoxon signed-rank tests were employed to analyze continuous clinical and imaging variables at baseline, discharge, and follow-up. To assess the association between LV reverse remodeling and various factors, univariate and multivariate logistic regression analyses were conducted. Cox proportional hazard regression models were employed to evaluate the prognostic value of LV reverse remodeling, and Kaplan–Meier curves were generated for the composite endpoint of hospitalization for heart failure and all-cause mortality.

For the second objective, Kruskal-Wallis tests were used to analyze the association between ILV and the number of valve positioning attempts during TAVI. Data were log-transformed due to non-normal distribution, and univariate linear regression analysis was performed to identify associations between risk factors and log-transformed ILV. Multivariate linear regression models were developed using the backward method. Predictors of periprocedural stroke were determined using uni- and multivariate logistic regression. Changes in neurocognition over time were assessed through repeated-measures analysis of variance, with pairwise differences evaluated using Duncan’s multiple comparison test. Differences between discharge TAVI and 6M DTI scalar metrics (FA, AD, MD, AD) were evaluated using paired sample t-tests, with Bonferroni correction applied for the 7 ROI comparisons ($p < 0.0071$). Repeated measures analysis of variance (ANOVA) was used to assess the effects of sex, ILV, and age on DTI metric changes from discharge to 6M MRI, followed by post hoc tests with Bonferroni correction ($p < 0.0167$). Spearman correlation tests were performed to analyze the associations between DTI metrics in each ROI and cognitive results. For all statistical tests, a p-value < 0.05 was considered significant. SPSS software (version 23; IBM Corp.) was used for all calculations.

4 RESULTS

4.1 LV reverse remodelling study

In effect a total, 234 CTAs of 117 patients (mean age 79.0 ± 7.5 years, 53.8% female, mean BSA and mean BMI 26.9 ± 4.7 kg/m²) were included in the final analysis. 24.8% of the patients had prior myocardial infarction, 98.3% had hypertension and 78.6% had hyperlipidemia. Oral anticoagulant medication was administered in 30.8% of all cases. HALT was reported in 30/117 (25.6%) cases. All patients were successfully implanted with CoreValve (76.1%), Evolut R (16.2%), Portico (6.0%) or Lotus (1.7%) self-expandable valves.

4.1.1 Assessment of LV reverse remodelling after TAVI

LVM and LVMi decreased substantially following TAVI 180.5 ± 53.0 vs. 137.1 ± 44.8 g ($p < 0.001$) and 99.7 ± 25.4 vs. 75.4 ± 19.9 g/m² ($p < 0.001$) for pre- and post TAVI respectively).

We detected an average 43.4 grams reduction in LVM which corresponds to a 22.8 % change after TAVI. In 73/117 patients (62.4%) we found more than 20 % reduction in myocardial mass. We also found that patients with lesser LV reverse remodelling had significantly higher prevalence of SLT and prior myocardial infarction.

4.1.2 Predictors of LV reverse remodelling

We evaluated clinical and imaging parameters for association with LV reverse remodelling. We found that SLT was inversely and independently associated with LV remodelling over age, gender, prior myocardial infarction change in mean pressure gradient and traditional risk factors (hypertension, dyslipidaemia, body mass index, and diabetes mellitus) in multivariate logistic regression analysis; OR 0.27, $P = 0.022$ (Table 1). The number of leaflets affected by SLT did not show an association with reverse remodelling ($P = 0.391$).

Parameters	Univariate model		Multivariate model	
	OR	P value	OR	P value
ACE-I/ARB therapy	0.57	0.311		
Myocardial infarction in history	0.28	0.002	0.22	0.006
SLT	0.35	0.025	0.27	0.022
Atrial fibrillation	0.74	0.497		

Oral anticoagulant therapy	0.79	0.599		
Change in mean aortic transvalvular pressure gradient (10 Hgmm change)	1.52	0.002	1.51	0.004

Table 1. Predictors of LV reverse remodelling following TAVI.

4.1.3. Prognostic relevance of LV reverse remodelling

Over an average follow-up period of 2.6 years, a total of 13 adverse events were recorded, including 9 deaths and 4 hospitalizations due to heart failure. Patients who showed a reduction in left ventricular (LV) mass of more than 20% following TAVI demonstrated better event-free survival compared to those with a lower degree of reverse remodelling (Figure 2). The reduction in LV mass by more than 20% remained a significant independent predictor of event-free survival even after considering other relevant factors in the multi-variate analysis (HR: 0.27; p=0.0033).

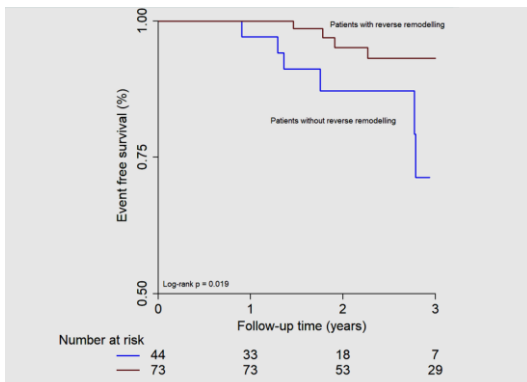


Figure 2. Kaplan Meier curve for mortality and repeat hospitalization following TAVI

4.2 Predictors and neurological consequences of periprocedural cerebrovascular events following TAVI

Among all patients, 113 patients were included in the analysis evaluating the periprocedural findings and complications (mean age 79.2 ± 6.7 years, 65.8% male, and mean BMI 27.3 ± 4.7 kg/m²). Overall, 23.9% (27/113) of the patients had prior myocardial infarction, 90.3% (102/113) had hypertension and 65.5% (74/113) had hyperlipidaemia. Oral anticoagulant medication was administered in 29.2% (33/113), while 74.3% (84/113) of the patients received antiplatelet therapy. Prosthetic valves were implanted successfully in all patients (Medtronic CoreValve 8.0%, Medtronic CoreValve Evolut R 66.3%, Portico 25.7%). Transfemoral approach was used in 105 cases (92.9%), transsubclavian access in 6 patients (5.3%), while transcarotid route in 2 cases (1.8%). Balloon predilatation was performed in 15 patients (15.3%), while most of the valves (78.8%) were postdilated. The mean number of positional attempts was 1.7 ± 0.9 . In 60 (53.1%) cases, the implantation was successful at the first positional attempt, in 39 (34.5%) cases at the second, and in 14 patients (12.4%) at the third or fourth time. According to the VARC-3 criteria 9 patients had major and 17 patients had minor vascular and access-related complications.

4.2.1 Cerebral embolization after TAVI

We detected new cerebral ischemic lesions on discharge brain MRI in 104 patients (92.0%) (Figure 3), among them 6 (5.3%) patients had periprocedural stroke. The median number of lesions per patient was 6 (IQR: 2-10), and the median ILV was 257.3 μ l (IQR: 97.1-718.8 μ l). 944 new ischemic brain lesions were found on brain MRI, most of the lesions were supratentorial (781/944, 81.9%), and the majority were located in the cortical subcortical area (796/944, 84.3%). On the follow-up 6M MRI 46/113 (40.7%) patients had gliotic transformation on FLAIR images. Most of the lesions were under 5 mm (558, 59.1%).

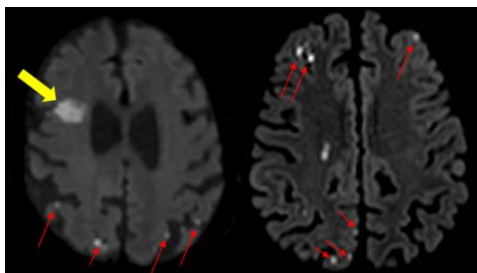


Figure 3. New ischemic lesion after TAVI.

4.2.2 Predictors of ischemic lesion volume and stroke after TAVI

Predictors of ischemic lesion volume and stroke after TAVI

In order to identify potential predictors of ILV and stroke, the association of various clinical and imaging parameters were investigated. Age, cardiovascular risk factors, aortic calcification, access route, valve type and size, and postdilatation did not show any association with ILV (all statistically non-significant, $p>0.05$). We found that sex, AVCS, number of valve positioning attempts, and predilatation showed association with log-transformed ILV in univariate analysis. AVCS was not an independent predictor of log-transformed ILV after adjustments. Regarding ILV, it seems that the manipulations during TAVI are more relevant than the aortic valve calcification: positioning the device three or more times resulted in a significant increase in ILV (Figure 4).

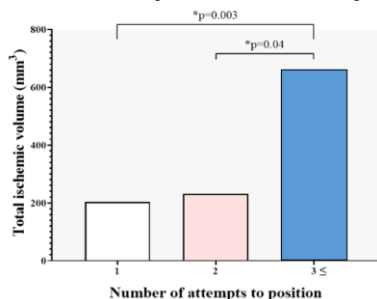


Figure 4. Total ischemic volume on MRI and the number of TAVI positioning attempts.

4.2.3 Changes in neurocognitive function

In total of 79/113 patients had serial neurocognitive assessment and post-TAVI MRI, these subjects were included in our subanalysis. The overall cognitive performance of the cohort was stable over the 1Y follow-up period, with mean baseline, discharge, 6M and 1Y Addenbrooke's scores of 72.3 ± 13.1 , 74.8 ± 14.2 , 72.8 ± 16.6 and 73.4 ± 13.4 , $p=0.32$ and MMS score: 25.9 ± 2.8 , 26.1 ± 3.5 , 25.8 ± 4.1 and 26.3 ± 3.0 , $p=0.92$, respectively

4.3 Assessment of DTI metric changes

In this substudy 78 subjects were included. 74 out of 78 study subjects (95%) had recent ischemic lesions with restricted diffusion, 71 of them supratentorial (91%), most of them multiple (57/70, 81%) ranging from 2-20 mm. 363 supratentorial lesions were found, more in the left cerebral hemisphere (194 vs 169). The

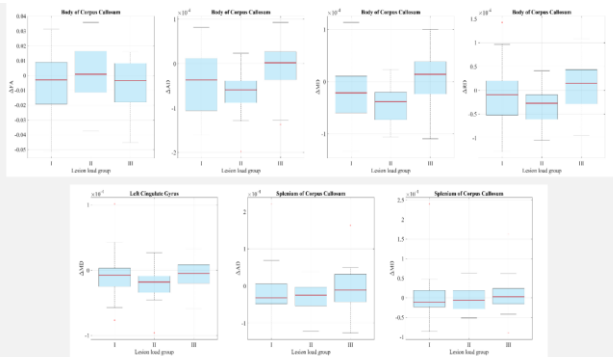
majority of these lesions were small (268/363, 74%, $\leq 5\text{mm}$; 109/363, 30%), mostly located at the cortical-subcortical region. The median lesion volume was 38.88 mm³ (range 14 mm³–17.4 cm³).

4.3.1 Analysis of DTI scalar metrics changes

In 4 out of the 7 WM ROIs significant reduction of AD was detected (genu and body; $p < 0.0001$; splenium and right parahippocampal cingulum: $p = 0.0023$), coupled with significant decrease of the MD in the body of corpus callosum ($p = 0.0006$) and FA in the splenium ($p < 0.0001$) using the paired sample t-test with Bonferroni-correction. We found significant reduction of RD and MD in the cingulate gyrus bilaterally significant reduction of RD and MD (right cingulate gyrus: MD - $p = 0.0025$, RD - $p = 0.0053$; left cingulate gyrus: MD - $p = 0.0004$, RD - $p = 0.0010$). The other changes were not significant.

4.3.2 Effects of ILV on DTI metric changes

The repeated measure ANOVA showed significant effect of ILV on certain DTI metric changes in 3 out of 7 ROIs. Figure 5. In the body of the corpus callosum the repeated measures ANOVA detected a significant effect of ILV on the change of AD, MD and RD across the groups ($p = 0.0045$, 0.0050, and 0.0175, respectively). As revealed by the post hoc comparison, the difference was the most pronounced between the ILV group I (decrease of AD and MD) and the ILV group III (increase of AD and MD); $p = 0.0183$ for AD and $p = 0.0457$ for MD. In group III the RD increased and the FA decreased (as opposed to groups I-II), without reaching the level of significance. In the left cingulate gyrus significant difference in MD reduction was found between the ILV group II and group III ($p = 0.0087$). The decrease of MD was more marked in the intermediate group relative to the group with the highest ILV. In the splenium of the corpus callosum the increase of MD differed significantly comparing group II with group III ($p = 0.0399$). The more pronounced increase in MD and a non-significant increase of AD in ILV group III versus the reduction of AD in groups I-II) point towards unfavorable microstructural alteration associated with higher ILV. The other associations were non significant.



AD = axial diffusivity; FA = fractional anisotropy; MD = mean diffusivity; RD = radial diffusivity
 Note: Metric dimensions: FA: dimensionless; MD, AD, RD: mm²/s

Figure 5. Box plots of association of change in diffusion tensor imaging metrics with ischemic lesion volume (ILV).

4.3.3 Cognitive trajectory

106 participants completed the pre-TAVI, 83 subjects the post-TAVI, 93 subjects the 6M, finally 79 patients the 1Y cognitive tests. Neurocognitive tests were completed in the DTI group in 51, 42, 57, 49 cases respectively. The Kruskal-Wallis test did not reveal a significant difference in the distribution of ACE and MMSE scores between the DTI and the non-DTI groups, and the corresponding boxplots showed a very similar trend in all cognitive domains, therefore we opted for analysing the cognitive performance of the whole study cohort.

Although there was an improvement in 3 domains and ACE score, the repeated-measures linear mixed-effect model revealed no significant change in cognitive function over one year. The pre-TAVI cognitive function had a significant effect on later scores at any timepoints ($p < 0.0001$): the lower the ACE score was prior to the intervention, the more pronounced improvement was observed after TAVI. In ILV group III there was a significant decline in retrograde memory ($p = 0.0489$) and visual scores ($p = 0.0151$) compared to ILV groups I+II. Apart from the improvement of evocation scores from pre-TAVI to post-TAVI, the Wilcoxon signed-rank test showed no significant change, in particular deterioration, regarding any domains across any different timepoints.

5 CONCLUSION

5.1 Adverse left ventricular remodelling and subclinical leaflet thrombosis following TAVI

Our study demonstrates the favorable long-term effects of TAVI on LV morphology using serial CT imaging. Our study provides insight into the interplay of HALT, reverse remodelling and clinical outcomes. We found that TAVI resulted a significant LVM regression on CT, and we demonstrated that the presence of SLT of the bioprosthetic valve and prior myocardial infarction might inhibit reverse remodelling process. Moreover, larger reverse remodelling following TAVI is associated with improved long-term prognosis and clinical outcome.

5.2 Predictors and neurological consequences of periprocedural cerebrovascular events after TAVI using MRI

We found that 92% of the patients had new cerebral ischemic lesions, however most of them were clinically silent. Balloon predilatation and the number of valve positioning attempts during the procedure were independently associated with a larger log-transformed ILV, whereas predilatation and alternative access route were associated with periprocedural stroke. The ILV was not associated with cognitive decline after TAVI.

5.3 Microstructural white-matter changes after TAVI using diffusion MRI

Significant effect of TAVI on cerebral microstructural properties was found with reduced diffusivities opposite to the general trends reported in studies of various neurodegenerative conditions and ageing, notably in women (in line with the lower cardiovascular risk revealed in females of our cohort) and lower ILV when comparing the result of the discharge brain MRI to 6M MRI results. Moreover, the overall cognitive function was maintained despite the high intrinsic ischemic load following TAVI with significant inverse relationship between ILV and cognitive scores in some domains.

6 BIBLIOGRAPHY OF THE CANDIDATE

6.1 Publication related to the present thesis

1. Bálint Szilveszter, Daniel Oren, Levente Molnár, Astrid Apor, Anikó I Nagy, Andrea Molnár, Borbála Vattay, Márton Kolossváry, Júlia Karády, Andrea Bartykowszki, Ádám L Jermendy, **Ferenc I Suhai**, Alexisz Panajotu, Pál Maurovich-Horvat, Béla Merkely, Subclinical leaflet thrombosis is associated with impaired reverse remodelling after transcatheter aortic valve implantation, *European Heart Journal - Cardiovascular Imaging*, Volume 21, Issue 10, October 2020, Pages 1144–1151 (**IF: 4,841**)

2. **Suhai FI**, Varga A, Szilveszter B, Nagy-Vecsey M, Apor A, Nagy AI, Kolossváry M, Karády J, Bartykowszki A, Molnár L, Jermendy AL, Panajotu A, Maurovich-Horvat P, Merkely B. Predictors and neurological consequences of periprocedural cerebrovascular events following transcatheter aortic valve implantation with self-expanding valves. *Front Cardiovasc Med.* 2022 Oct 5;9:951943. (IF: 5,05). Lin A, Vecsey-Nagy M, et al. The effect of patient and imaging characteristics on coronary CT angiography assessed pericoronary adipose tissue attenuation and gradient. *Journal of Cardiovascular Computed Tomography.* 2022. IF: 5,17
3. Boussoussou M, Varga A, Gyebnár G, **Suhai FI**, Nagy AI, Kozák LR, Póka CÁ, Turáni MF, Borzsák S, Apor A, Bartykowszki A, Szilveszter B, Kolossváry M, Maurovich-Horvat P, Merkely B. Microstructural alterations measured by diffusion tensor imaging following transcatheter aortic valve replacement and their association with cerebral ischemic injury and cognitive function - a prospective study. *Neuroradiology.* 2022 Dec;64(12):2343-2356. (IF: 2,98)

6.2 Bibliography not related to the present thesis

1. Szilveszter B, Nagy AI, Vattay B, Apor A, Kolossváry M, Bartykowszki A, Simon J, Drobní ZD, Tóth A, Suhai FI, Merkely B, Maurovich-Horvat P. Left ventricular and atrial strain imaging with cardiac computed tomography: Validation against echocardiography. *J Cardiovasc Comput Tomogr.* 2020 Jul-Aug;14(4):363-369.
2. Karády J, Apor A, Nagy AI, Kolossváry M, Bartykowszki A, Szilveszter B, Simon J, Molnár L, Jermendy AL, Panajotu A, Suhai FI, Varga A, Rajani R, Maurovich-Horvat P, Merkely B. Quantification of hypo-attenuated leaflet thickening after transcatheter aortic valve implantation: clinical relevance of hypo-attenuated leaflet thickening volume. *Eur Heart J Cardiovasc Imaging.* 2020 Dec 1;21(12):1395-1404.
3. Vágó H, Szabó L, Dohy Z, Czibalmos C, Tóth A, Suhai FI, Bérczi G, Gyarmathy VA, Becker D, Merkely B. Early cardiac magnetic resonance imaging in troponin-positive acute chest pain and non-obstructed coronary arteries *Heart.* 2020 Jul;106(13):992-1000.
4. Dohy Z, Vereckei A, Horvath V, Czibalmos C, Szabo L, Toth A, Suhai FI, Csécs I, Becker D, Merkely B, Vago H. How are ECG parameters related to cardiac magnetic resonance images? Electrocardiographic predictors of left ventricular hypertrophy and myocardial fibrosis in hypertrophic cardiomyopathy. *Ann Noninvasive Electrocardiol.* 2020 Sep;25(5):e12763.
5. Maurovich-Horvat P, Károlyi M, Horváth T, Szilveszter B, Bartykowszki A, Jermendy AL, Panajotu A, Celeng C, Suhai FI, Major GP, Csobay-Novák C, Hüttl K, Merkely B. Esmolol is noninferior to metoprolol in achieving a target heart rate of 65 beats/min in patients referred to coronary CT angiography: a randomized controlled clinical trial. *J Cardiovasc Comput Tomogr.* 2015 Mar-Apr;9(2):139-45. doi: 10.1016/j.jcct.2015.02.001. Epub 2015 Feb 14. PMID: 25819196.

6. Csecs I, Czibalmos C, Suhai FI, Mikle R, Mirzahosseini A, Dohy Z, Szücs A, Kiss AR, Simor T, Tóth A, Merkely B, Vágó H. Left and right ventricular parameters corrected with threshold-based quantification method in a normal cohort analyzed by three independent observers with various training-degree. *Int J Cardiovasc Imaging*. 2018 Jul;34(7):1127-1133.
7. Czibalmos C, Csecs I, Toth A, Kiss O, Suhai FI, Sydó N, Dohy Z, Apor A, Merkely B, Vago H. The demanding grey zone: Sport indices by cardiac magnetic resonance imaging differentiate hypertrophic cardiomyopathy from athlete's heart. *PLoS One*. 2019 Feb 14;14(2):e0211624.
8. Czibalmos C, Csecs I, Dohy Z, Toth A, Suhai FI, Müssigbrodt A, Kiss O, Geller L, Merkely B, Vago H. Cardiac magnetic resonance based deformation imaging: role of feature tracking in athletes with suspected arrhythmogenic right ventricular cardiomyopathy. *Int J Cardiovasc Imaging*. 2019 Mar;35(3):529-538.
9. Csecs I, Czibalmos C, Toth A, Dohy Z, Suhai IF, Szabo L, Kovacs A, Lakatos B, Sydó N, Kheirkhahan M, Peritz D, Kiss O, Merkely B, Vago H. The impact of sex, age and training on biventricular cardiac adaptation in healthy adult and adolescent athletes: Cardiac magnetic resonance imaging study. *Eur J Prev Cardiol*. 2020 Mar;27(5):540-549.
10. Székely M, RuttKay T, Suhai FI, Bóna Á, Merkely B, Székely L. Minimally invasive apical cannulation and cannula design for short-term mechanical circulatory support devices. *BMC Cardiovasc Disord*. 2022 Sep 4;22(1):395.
11. Apor A, Bartykowska A, Szilveszter B, Varga A, Suhai FI, Manouras A, Molnár L, Jermendy ÁL, Panajotu A, Turáni MF, Papp R, Karády J, Kolossváry M, Kovács T, Maurovich-Horvat P, Merkely B, Nagy AL. Subclinical leaflet thrombosis after transcatheter aortic valve implantation is associated with silent brain injury on brain magnetic resonance imaging. *Eur Heart J Cardiovasc Imaging*. 2022 Nov 17;23(12):1584-1595.
12. Szücs A, Kiss AR, Suhai FI, Tóth A, Gregor Z, Horváth M, Czibalmos C, Csécs I, Dohy Z, Szabó LE, Merkely B, Vágó H. The effect of contrast agents on left ventricular parameters calculated by a threshold-based software module: does it truly matter? *Int J Cardiovasc Imaging*. 2019 Sep;35(9):1683-1689.
13. Maurovich-Horvat P, Suhai FI, Czibalmos C, Tóth A, Becker D, Kiss E, Ferencik M, Hoffmann U, Vágó H, Merkely B. Coronary Artery Manifestation of Ormond Disease: The "Mistletoe Sign". *Radiology*. 2016 Aug 22;160644.
14. Vecsey-Nagy M, Jermendy ÁL, Kolossváry M, Vattay B, Boussoussou M, Suhai FI, Panajotu A, Csöre J, Borzsák S, Fontanini DM, Csobay-Novák C, Merkely B, Maurovich-Horvat P, Szilveszter B. Heart Rate-Dependent Degree of Motion Artifacts in Coronary CT Angiography Acquired by a Novel Purpose-Built Cardiac CT Scanner. *J Clin Med*. 2022 Jul 26;11(15):4336.
15. Szabó L, Juhász V, Dohy Z, Fogarasi C, Kovács A, Lakatos BK, Kiss O, Sydó N, Csulak E, Suhai FI, Hirschberg K, Becker D, Merkely B, Vágó H. Is cardiac involvement prevalent in highly trained athletes after SARS-CoV-2 infection? A

- cardiac magnetic resonance study using sex-matched and age-matched controls *Br J Sports Med.* 2022 May;56(10):553-560.
16. Vecsey-Nagy M, Jermendy AL, Suhai FI, Panajotu A, Csöre J, Borzsák S, Fontanini DM, Kolossváry M, Vattay B, Boussousou M, Csobay-Novák C, Merkely B, Maurovich-Horvat P, Szilveszter B. Model-based adaptive filter for a dedicated cardiovascular CT scanner: Assessment of image noise, sharpness and quality. *Eur J Radiol.* 2021 Dec;145:110032.
 17. Szűcs A, Kiss AR, Gregor Z, Horváth M, Tóth A, Dohy Z, Szabó LE, Suhai FI, Merkely B, Vágó H. Changes in strain parameters at different deterioration levels of left ventricular function: A cardiac magnetic resonance feature-tracking study of patients with left ventricular noncompaction. *Int J Cardiol.* 2021 May 15;331:124-130.
 18. Budai A*, Suhai FI*, Csorba K, Toth A, Szabo L, Vago H, Merkely B. Fully automatic segmentation of right and left ventricle on short-axis cardiac MRI images *Comput Med Imaging Graph.* 2020 Oct;85:101786.
 19. Tokodi M, Staub L, Budai A, Lakatos BK, Csákvári M, Suhai FI, Szabó L, Fábrián A, Vágó H, Tösér Z, Merkely B, Kovács A. Partitioning the Right Ventricle Into 15 Segments and Decomposing Its Motion Using 3D Echocardiography-Based Models: The Updated ReVISION Method. *Front Cardiovasc Med.* 2021 Mar 4;8:622118.
 20. Ádám Budai; Ferenc Imre Suhai; Kristof Csorba; Zsófia Dohy; Liliana Szabo; Bela Merkely; Hajnalka Vago. Automated Classification of Left Ventricular Hypertrophy on Cardiac MRI. *Applied Sciences Appl. Sci.* 2022, 12, 4151.
 21. Szegedi N, Suhai IF, Perge P, Salló Z, Hartyánszky I, Merkely B, Gellér L J Atrio-esophageal fistula clinically presented as pericardial-esophageal fistula. *Interv Card Electrophysiol.* 2021 Sep;61(3):623-624.
 22. Székely R, Suhai FI, Karlinger K, Baksa G, Szabaczki B, Bárány L, Pölöskei G, Rácz G, Wagner Ö, Merkely B, Ruttkay T. Human Cadaveric Artificial Lung Tumor-Mimic Training Model. *Pathol Oncol Res.* 2021 Apr 26;27:630459.
 23. Vattay B, Borzsák S, Boussousou M, Vecsey-Nagy M, Jermendy AL, Suhai FI, Maurovich-Horvat P, Merkely B, Kolossváry M, Szilveszter B. Association between coronary plaque volume and myocardial ischemia detected by dynamic perfusion CT imaging. *Front Cardiovasc Med.* 2022 Sep 8;9:974805.
 24. Vago H, Czibalmos C, Papp R, Szabo L, Toth A, Dohy Z, Csecs I, Suhai F, Kosztin A, Molnar L, Geller L, Merkely B. Biventricular pacing during cardiac magnetic resonance imaging. *Europace.* 2020 Jan 1;22(1):117-124.
 25. Dohy Z, Szabo L, Toth A, Czibalmos C, Horvath R, Horvath V, Suhai FI, Geller L, Merkely B, Vago H. Prognostic significance of cardiac magnetic resonance-based markers in patients with hypertrophic cardiomyopathy. *Int J Cardiovasc Imaging.* 2021 Jun;37(6):2027-2036.
 26. Şulea CM, Lakatos B, Kovács A, Benke K, Suhai FI, Csulak E, Merkel E, Nagy B, Hartyánszky I, Merkely B, Szabolcs Z, Pólos M. Blood-filled cyst of the

- tricuspid valve: Multiple cardiac disorders, one surgical case. *J Card Surg.* 2022 Jan;37(1):245-248.
27. Csulak E, Petrov Á, Kováts T, Tokodi M, Lakatos B, Kovács A, Staub L, Suhai FI, Szabó EL, Dohy Z, Vágó H, Becker D, Müller V, Sydó N, Merkely B. The Impact of COVID-19 on the Preparation for the Tokyo Olympics: A Comprehensive Performance Assessment of Top Swimmers. *Int J Environ Res Public Health.* 2021 Sep 16;18(18):9770.
 28. Dohy Z, Szabo L, Pozsonyi Z, Csécs I, Toth A, Suhai FI, Czibalmos C, Szucs A, Kiss AR, Becker D, Merkely B, Vago H. Potential clinical relevance of cardiac magnetic resonance to diagnose cardiac light chain amyloidosis. *PLoS One.* 2022 Jun 13;17(6):e0269807.
 29. Csöre J, Suhai FI, Gyánó M, Pataki ÁA, Juhász G, Vecsey-Nagy M, Pál D, Fontanini DM, Bérczi Á, Csobay-Novák C. Quiescent-Interval Single-Shot Magnetic Resonance Angiography May Outperform Carbon-Dioxide Digital Subtraction Angiography in Chronic Lower Extremity Peripheral Arterial Disease. *J Clin Med.* 2022 Aug 1;11(15):4485.
 30. Jermendy, G., Kolosváry, M., Dudás, I., Jermendy, Á. L., Panajotu, A., Suhai, I. F., Drobní, Z. D., Karády, J., Tárnoki, Á. D., Tárnoki, D. L., Voros, S., Merkely, B., & Maurovich-Horvat, P.. Effect of genetic and environmental influences on hepatic steatosis: A classical twin study based on computed tomography, Imaging, 12(1), 15-20. (2020)
 31. Orbán G, Dohy Z, Suhai FI, Nagy AI, Salló Z, Boga M, Kiss M, Kunze K, Neji R, Botnar R, Prieto C, Gellér L, Merkely B, Vágó H, Szegedi N. Use of a new non-contrast-enhanced BOOST cardiac MR sequence before electrical cardioversion or ablation of atrial fibrillation-a pilot study. *Front Cardiovasc Med.* 2023 Jun 16;10:1177347.
 32. Mihály Zsuzsanna, László Hidi, Ferenc Suhai, Zsófia Tarcza, Balázs Nemes, Péter Sótónyi. Nyaki verőér atípusos, fokális, fibromuscularis dysplasiájának képalkotó diagnosztikai nehézségei *MAGYAR RADIOLÓGIA* 2020; 94 : 1-2 pp. 70-74.
 33. Vágó H , Tóth A , Czibalmos Cs , Suhai FI , Kecskés K , Heltai K , Zima E , Bérczi Gy , Simor T , Becker D , Merkely B. Culpit lézió nélküli ST-elevációs miokardiális infarktus differenciáldiagnosztikája szív mágneses rezonanciavizsgálattal segítségével *Cardiologia Hungarica* 2014; 44:300-305.
 34. Suhai Ferenc Imre, Sax Balázs, Assabiny Alexandra, Király Ákos, Czibalmos Csilla, Csécs Ibolya, Kovács Attila, Latakos Bálint, Németh Endre, Becker Dávid, Szabolcs Zoltán, Hubay Márta, Merkely Béla, Vágó Hajnalka. A szív MR-vizsgálat szerepe kevert típusú (humorális és celluláris) kardialis allograft rejección esetén. *Cardiologia Hungarica* 2018; 48:44-51.
 35. Juhász G, Csöre J, Suhai FI, Gyánó M, Pataki Á, Vecsey-Nagy M, Pál D, Fontanini DM, Bérczi Á, Csobay-Novák C. A kontrasztanyag nélküli mágnesesrezonancia-angiográfia diagnosztikus teljesítménye alsó végtagi verőérbetegekben. *Orv Hetil.* 2022 Nov 6;163(45):1782-1788.

36. Hidi L, Csobay-Novák C, Juhász V, Suhai F, Szeberin Z, Sótanyi P. Postdissectió aortaaneurysma endovasculáris kezelése „candy-plug” technikával perzisztáló állumen esetén. *Orv Hetil.* 2020 Mar;161 (11):437-439.
37. Csécs Ibolya, Czibalmos Csilla, Tóth Attila, Kiss Orsolya, Komka Zsolt, Bárczi György, Kovács Tímea, Suhai Ferenc Imre, Sydó Nóra, Simor Tamás, Gellér László, Becker Dávid, Merkely Béla, Vágó Hajnalka. Sportszív vagy strukturális szívizombetegség? Szív mágneses rezonanciás vizsgálat diagnosztikus szerepe sportolóknál strukturális szívbetegség gyanúja esetén. *Cardiologia Hungarica* 2017; 47:10-17.
38. Kádár Krisztina, Csöre Judit, Liptai Csilla, Tóth Attila, Kovács Attila, Molnár Levente, Suhai Imre, Assabiny Alexandra, Kuthi Luca, Édes István, Kertész Attila Béla, Merkely Béla, Hartvánszky István. Kawasaki-betegség gyermekkorától a felnőttkorig. Multimodális képalkotók szerepe a hosszú távú nyomonkövetésben. *Cardiologia Hungarica* 2017; 47:243-249.
39. Borbóla József, Sári Csaba, Som Zoltán, Suhai Ferenc, Csepregi András. Miért érdemes a Fradinak szurkolni a Groupama Arénában? *Cardiologia Hungarica* 2020; 50: 444–450.
40. Dohy Zsófia, Csécs Ibolya, Czibalmos Csilla, Suhai Ferenc Imre, Tóth Attila, Szabó Liliána, Pozsonyi Zoltán, Simor Tamás, Merkely Béla, Vágó Hajnalka. Balkamra-hipertrofiával, illetve megnövekedett falvastagsággal járó cardiomyopathiák szív mágneses rezonanciás jellegzetességei. *Cardiologia Hungarica* 2018; 48: 390-396.
41. A szív mágneses rezonanciás vizsgálatának szerepe lezajlott COVID-19-fertőzést követően Szabó Liliána, Juhász Vencel, Dohy Zsófia, Hirschberg Kristóf, Czibalmos Csilla, Tóth Attila, Suhai Ferenc Imre, Merkely Béla, Vágó Hajnalka *Cardiologia Hungarica* 2021; 51: 18–22.
42. Hirschberg Kristóf, Dohy Zsófia, Tóth Attila, Szabó Liliána, Czibalmos Csilla, Finster Marius, Suhai Ferenc, Merkely Béla, Vágó Hajnalka. A mappingtechnikák által nyújtott lehetőségek a szív-MR-vizsgálatok során: indikációk, diagnosztikus érték, limitációk és centrumunk kezdeti tapasztalatai *Cardiologia Hungarica* 2020; 50: 45–53.